J. Fluid Mech. (1986), *vol.* 173, *pp.* 43–53
Printed in Great Britain

Acoustic monitoring of ocean gyres

By WALTER MUNK

Scripps Institution of Oceanography, University of California,
San Diego, La Jolla, CA 92093, USA

(Received 12 February 1986)

There has been an increased interest in ocean phenomena with horizontal scales comparable to the radius of the Earth, and timescales of years and beyond. These phenomena occur in the presence of intense processes of higher spatial and temporal frequency. An observational programme for the large-scale phenomena has an inherent advantage if it can rely on measurements that are, by their very nature, integrated moments over the prerequisite scale.

The oceans provide an excellent medium for transmitting sound waves of low frequency, as demonstrated in the closing days of World War II, and subsequently confirmed by a 20000 km acoustic transmission between Perth, Australia and Bermuda. For the last six years we have been developing a method (Ocean Acoustic Tomography) to take advantage of the favourable ocean acoustic properties. We measure travel time Δ^+ from mooring m to mooring n (positive x), and Δ^- from n to m. The sum $\Delta^+ + \Delta^-$ then gives information about the sound speed C (e.g. temperature) averaged along the acoustic ray path; the difference $\Delta^+ - \Delta^-$ gives information about the x-component u of current velocity. The recorded acoustic signal can be decomposed into 10–20 distinct ray arrivals Δ_i, each with a distinct ray path and associated depth-weighting of the ocean column; the ray travel times can be inverted to yield information about the depth profiles $C(z)$ and $u(z)$. The product $\langle C \rangle \langle u \rangle$ of these range-averaged quantities is related to the climatological large-scale heat flux; the space–time average $\overline{\langle \delta C\, \delta u \rangle}$ is related to the eddy heat flux, and can be estimated by measuring the difference variance $(\Delta^+) -$ variance (Δ^-).

1. Introduction

For 45 years I have looked to G. I. Taylor's work as a model for how to study fluids. Yet, in response to the conveners of this symposium, I had to reply that I was unable to come up with any contribution that would adequately illustrate the spirit of G. I. Taylor. George Batchelor put my fears to rest: 'If every contribution was required to be something which G.I might have done or which illustrates how he would have done it, the programme would be sparse indeed'. He then reminded me of G.I.'s early work on the ice-scout ship *Scotia* off the banks of Newfoundland. I have reread some of the early work, particularly the 1915 paper (the first of the collected *Scientific Papers*), when Taylor inferred the eddy motion in the lower atmosphere, and the transfer of heat and momentum through the atmospheric boundary layer, from just a few kite ascents. Based on this reading and from discussions with G.I. over the years on various oceanographic topics, I have concluded that G.I. would have enjoyed being aboard the *Oceanus* seventy years after the *Scotia* and twenty degrees to the south, inferring the ocean eddy structure from measurements at just a few moorings. But the comparison stops there; we cannot claim any resemblance between our elaborate acoustic equipment and the elegant simplicity of G.I.'s kites.

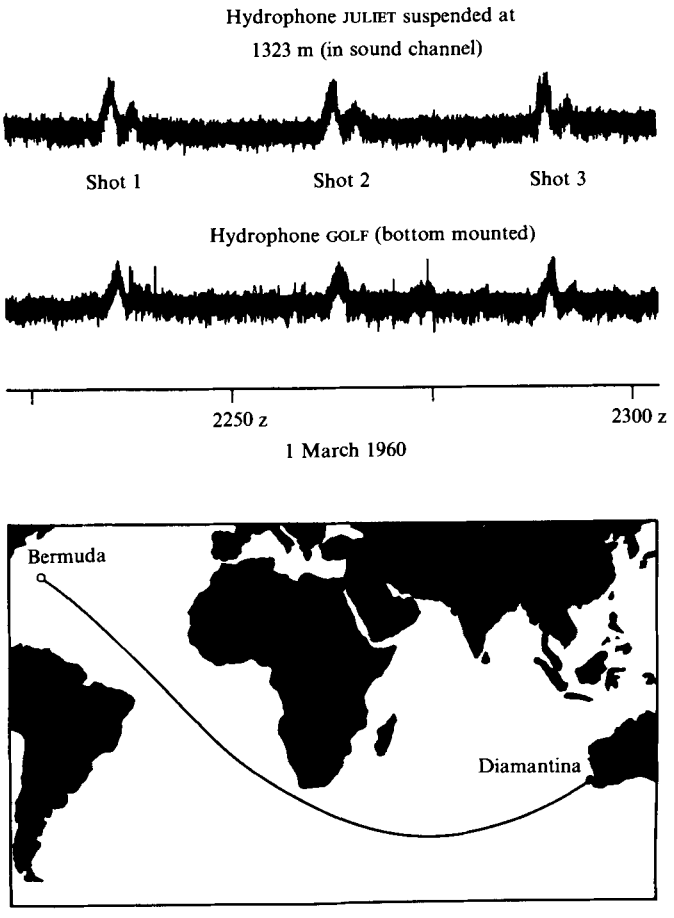

FIGURE 1. Bermuda oscillograms from detonation site off Perth, Australia, at a great circle range of 20000 km. Travel times were 3 h 42 min. From Shockley *et al.* (1982).

2. Global acoustics

Figure 1 shows a signal received in Bermuda from detonations off Perth, Australia, over a great circle path of 20000 km (Shockley, Northrop & Hansen, 1982). This experiment served as a dramatic demonstration of the effective propagation of low-frequency sound waves in the oceans. The realization, during the last decade or two, of an intense ocean-eddy scale of order 100 km poses a formidable challenge to the point-by-point mapping by traditional ship-board methods. The question naturally arises whether one can take advantage of the favourable acoustic properties of the oceans to measure the 'average effect of a collection of eddies' rather than 'the behaviour of eddies considered as individuals' (Taylor 1915).

3. A reciprocal transmission experiment

We report some of the results from an experiment conducted at 32° N, 70° W in 1983. (For a more complete discussion see Worcester, Spindel & Howe 1985 and Howe, Worcester & Spindel 1986.) Figure 2 shows the sound-speed profiles and all resolved ray paths. Figure 3 shows the measured and computed arrival patterns.

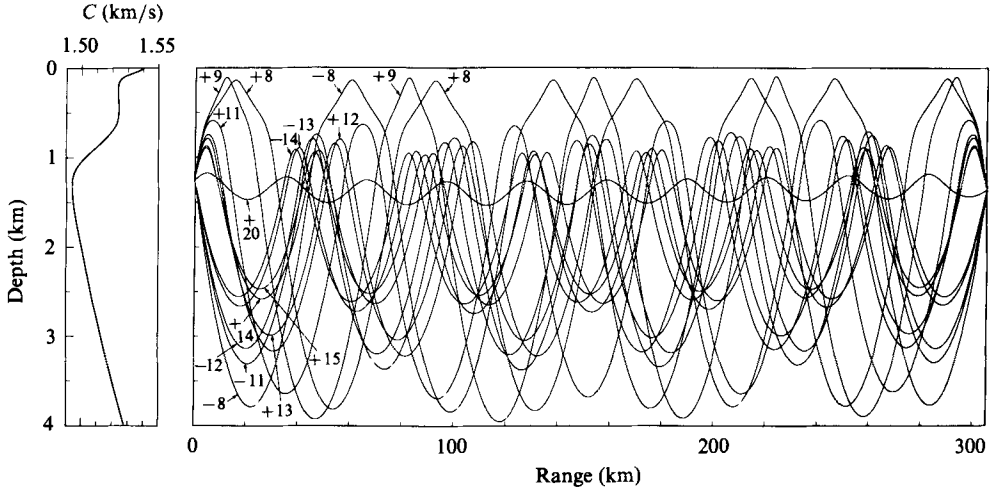

FIGURE 2. The mean sound-speed profile $C(z)$ (left) and the resolved 13 rays (right). The inversion of $C(z)$ between 200 and 600 m is associated with the layer of quite uniform 18 °C water.

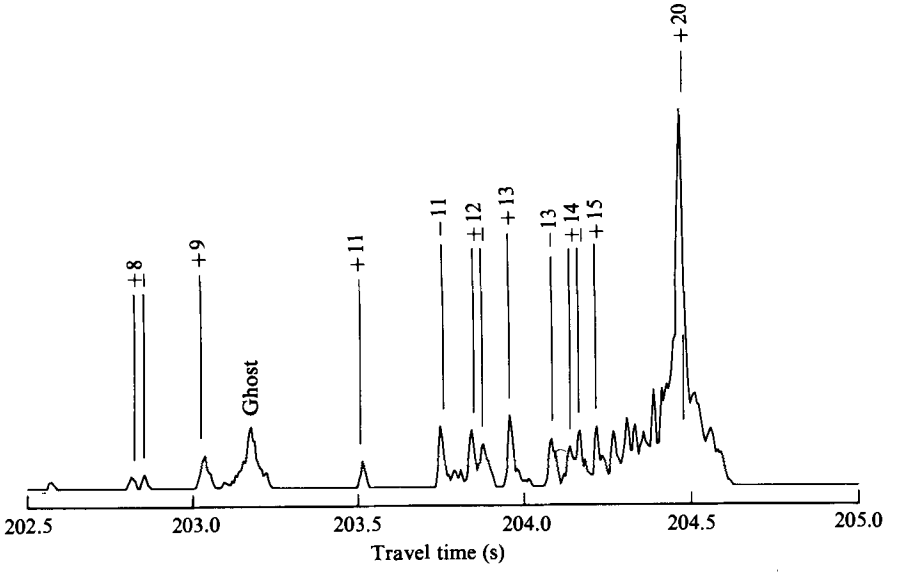

FIGURE 3. Measured and computed ray arrivals on year day 218. The close agreement is somewhat misleading (see text). The ghost arrival is associated with equipment nonlinearity.

Steep ray paths arrive early, flat (axial) paths arrive late. The steep rays have further to go, but this is more than compensated by the larger sound speed in the upper and lower ocean relative to the axial ocean. One may interpret the 'measured' arrival pattern as being the result of a single pulse of 10 ms duration. (In fact, the source emitted an extended coded signal with a unique pulse-like autocovariance, and the 'measured' signal is the covariance of the received signal with a stored replica of the source code.) The near-perfect agreement between measured and computed arrival times has to be interpreted with caution. The $C(x, z)$-field used in the construction of the rays is based on the complete available dataset, consisting of 18 XBT profiles, climatological information about salinities and about temperature in the ocean, *plus*

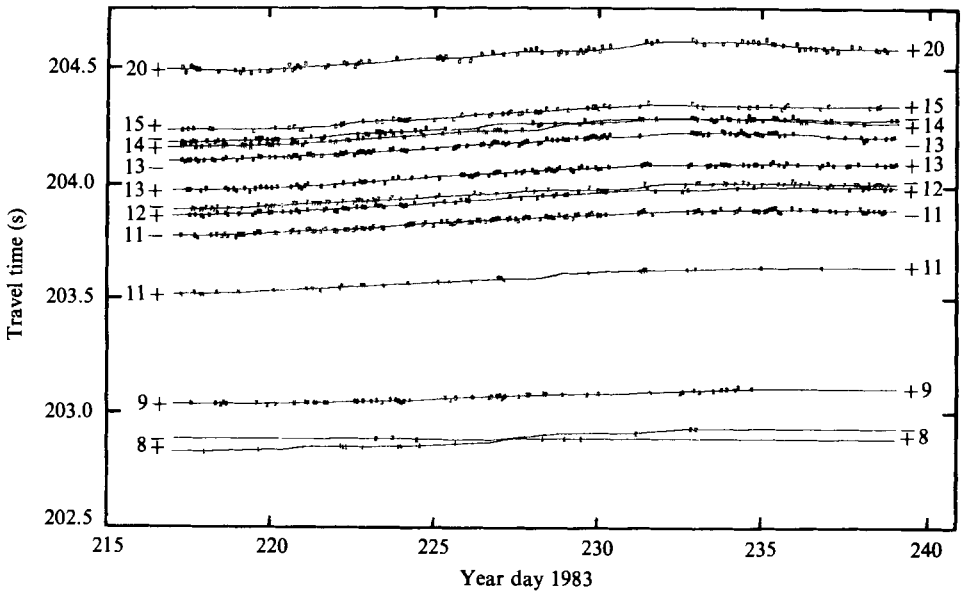

FIGURE 4. Ray travel times as a function of clock time for the resolved 13 rays.

the acoustic information. The important consideration is that the derived $C(x, z)$-field is consistent within the known experimental error limits of both the oceanographic and acoustic data. It differs only slightly (but permissibly) from the field one would have constructed using only the oceanographic data. (See figure 2 for the range-averaged $C(z)$.)

Our interest is in the variations with time subsequent to year day 218, as inferred from the acoustic data only. This consists of the travel times $\Delta_i(t)$ of 13 selected rays (figure 4), $i = 1$ to 13. The denseness and distribution of rays within this vertical section gives one some appreciation of the expected resolution. The experiment consisted of colocated sources and receivers at each of the two moorings. In this way we can form the sum $\Delta_i^+ + \Delta_i^-$ and difference $\Delta_i^+ - \Delta_i^-$ of reciprocal transmissions. The sum travel times give information about the variable sound speed $C_i(t)$ along ray i; fluctuations during the course of the experiment are of order 100 ms and easily measured. The difference travel times and their variations are both of order 10 ms and can be adequately measured; they give information about current component $u_i(t)$ averaged along ray path i. For a triangle of moorings, one can measure the 'sing-around' travel times clockwise and anticlockwise, and forming the difference one gets a measure of the vorticity within the array (Rossby 1975). Longuet-Higgins (1982) has considered some of the geometric properties of more elaborate arrays.

Different ray paths give different weighting to various depths. Flat rays see only the axial oceans (near 1300 m). Steep rays form an average over the depth range contained between the upper and lower turning points, with rather more weighting to the turning depths. For illustration consider an ocean model that consists of layers j with sound speed C_i. (See Howe *et al.* 1986 for the actual procedure.) Thus $\Delta_i = \sum_j R_{ij}/C_j$, where R_{ij} is the distance travelled by ray i in layer j. The linear inverse problem is to obtain the layer velocity C_j as a weighted sum of the dataset Δ_i. This can formally be written in terms of the inverse matrix R_{ij}^{-1}:

$$C_j = \sum_i R_{ij}^{-1} \Delta_i.$$

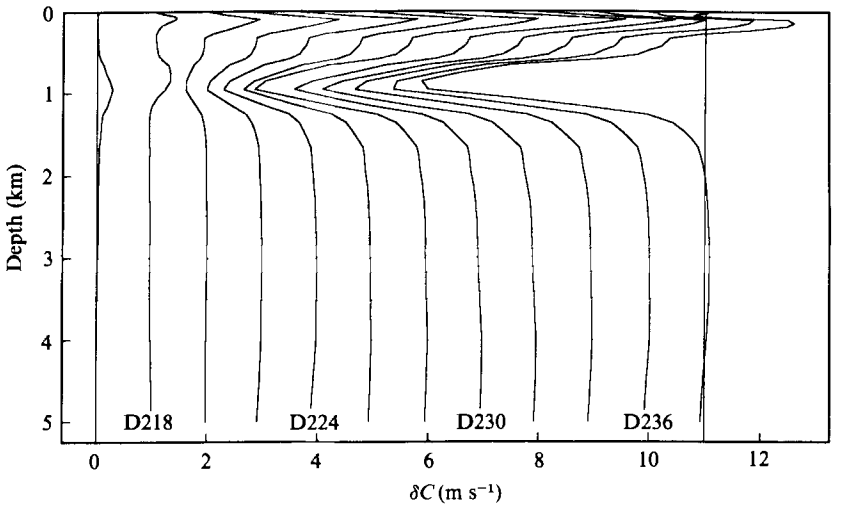

FIGURE 5. Departures in sound-speed profile $\delta C(z)$ at 2-day intervals, as inferred from the acoustic transmissions. The profiles are relative to the reference profile shown to the left on figure 2. The zero line is shifted to the right by 1 m s^{-1} on successive profiles.

One generally enters with more unknown parameters than data, and the inversion needs to be made unique by imposing restraints (such as finding the least wiggly field consistent with the dataset). It is preferable to use $\frac{1}{2}(\Delta_i^+ + \Delta_i^-)$ in the place of Δ_i in the above equation.

4. Variability in $C(z)$

Figure 5 shows the successive departures of the range-averaged $C(z)$ from the profile on year day 218. The principal feature is a decreasing sound speed by almost 5 m s^{-1} in 20 days (corresponding to a cooling by 1 °C) centred at 1 km depth. The development is not a surprise; in fact, the timescale, structure and magnitude of this variation is about what one would expect from a typical mesoscale activity in this region.

5. Variability in $u(z)$

A similar plot of successive current profiles (figure 6) shows an increasing negative velocity (towards SW) during the same 20 days. The gradient $\mathrm{d}u/\mathrm{d}z$ is largest near 1 km, the depth of maximum $C(z)$ variability. The deep current is nearly uniform in magnitude and increases from about 1 cm s^{-1} to 7 cm s^{-1} during the 20-day interval.

6. Modal representation

The uniformity of the deep current suggests the development of a barotropic current mode, and the usefulness of decomposing $C(z)$ and $u(z)$ into a (variable) modal structure. Figure 7 shows the associated wave functions for the barotropic ($m = 0$) and the gravest two baroclinic modes ($m = 1, 2$); m gives the number of zero crossings of the u wave function.

The variable amplitudes of the wave modes can be obtained directly from the inversion procedure. The results are shown in figure 8. The barotropic mode makes

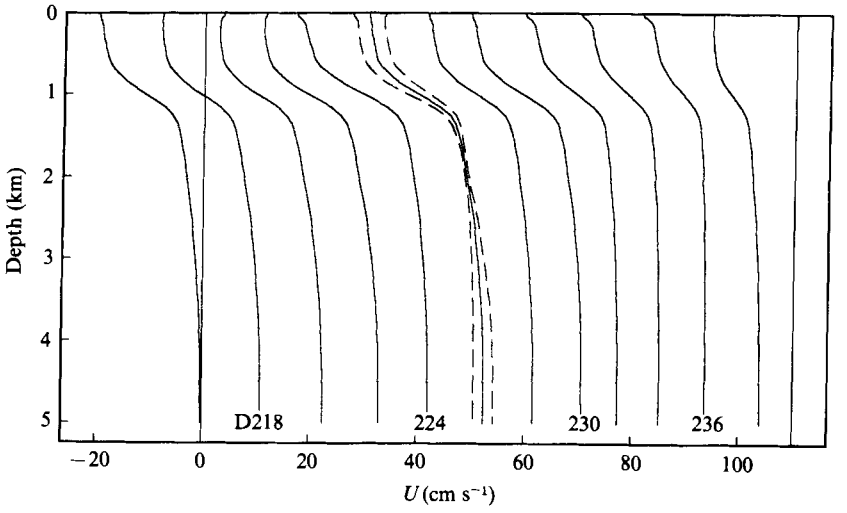

FIGURE 6. Current profiles $u(z)$ at 2-day intervals as inferred from the reciprocal transmissions. The zero line is shifted to the right by 10 cm s^{-1} on successive profiles. Error limits are indicated for year day 226.

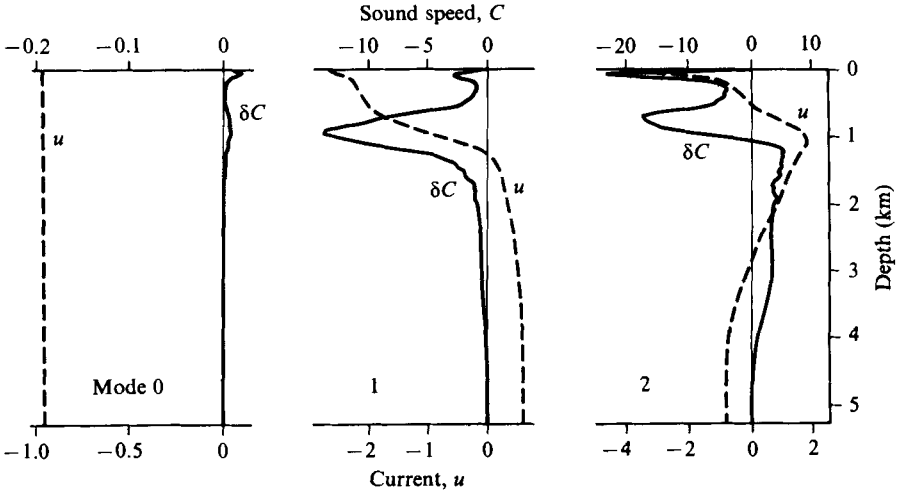

FIGURE 7. Normalized wave functions in vertical displacement, or C (solid) and horizontal velocity u (dashed) for modes 0, 1 and 2. The structure above 500 m depth is associated with the layer of 18 °C water (figure 2).

a negligible contribution to $C(z)$. The baroclinic mode 1 (whose wave function is peaked at 1 km depth) accounts for nearly all of the variation (relative to year day 218) of $C(z)$, but there is a small mode-2 contribution starting year day 233. Mode 2 makes a negligible contribution to the current. The situation changes from an early baroclinically dominated regime (about 2:1) to a late barotropic regime (about 3:1).

The C-modes (vertical displacement) and u-modes (horizontal velocity) could have been combined into a single modal representation if information had been available on both the x- and the y-component of the current.

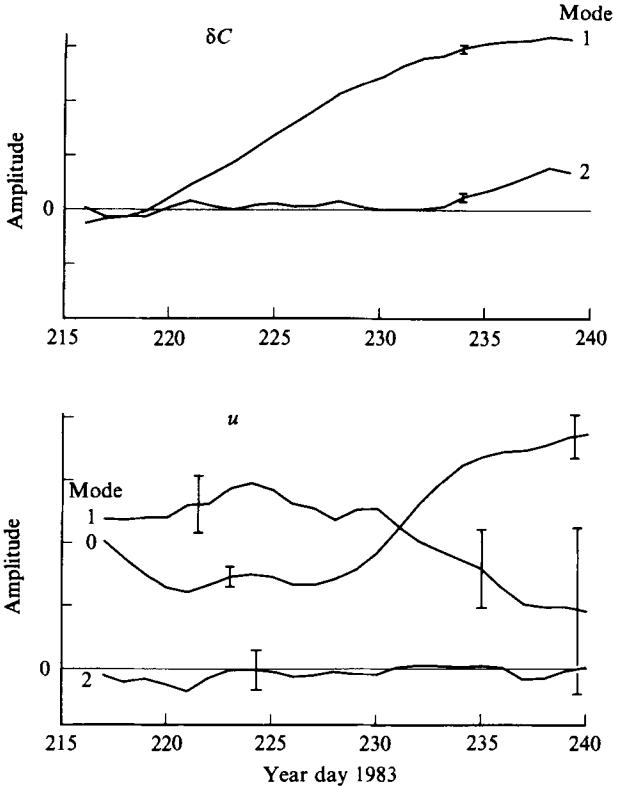

FIGURE 8. Variable amplitudes of the δC-modes (top) and u-modes (bottom) whose wave functions were shown in figure 7. Mode 0 (barotropic) makes a negligible contribution to vertical displacement (or δC). Error bars are shown.

7. Range resolution

We have been concerned with the range-averaged vertical profiles $C(z)$ and $u(z)$. But the acoustic travel times Δ_i for a single source–receiver pair provide some limited information about the range-dependent sound field. This is evident from the distribution of rays in the (x, z)-plane (figure 2); e.g. a shallow feature at 50 km range would not affect any rays, whereas at 100 km it would affect +8 and +9. (Clearly a three-dimensional array (Ocean Tomography Group 1982) has x, y, z resolution.) Write $C(x, z) = C_0(z) + \delta C(x, z)$, with $\langle \delta C(x, z) \rangle = 0$ for the range-averaged perturbation. Take the case of an integral number of double loops (like ± 14 in figure 2) with source and receiver at the same depth. In a range-independent ocean the rays with positive (+) and negative (−) launch angles have precisely the same travel times. A split arrival is then the result of range dependence, and can give some information about range dependence. But this is just a special case; some information on the x-dependence is contained in all ray arrival times. Malanotte-Rizzoli (1985) has demonstrated satisfactory results in deriving the linear and quadratic x-trend. The ability to resolve smaller features depends on the noise level. For the 1983 experiment the results look quite promising (figure 9).

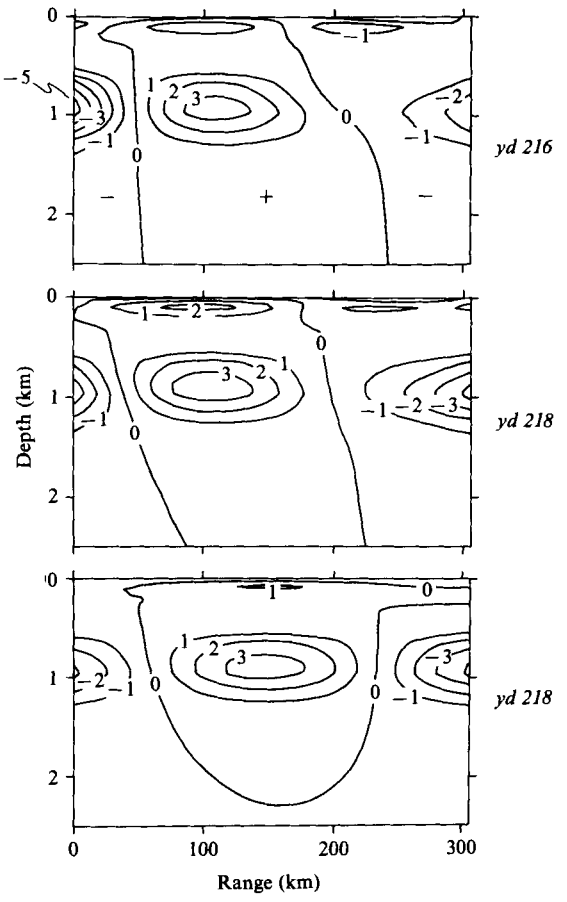

FIGURE 9. Contours (in m s^{-1}) of range-dependent departure $\delta C(x, z)$ relative to the reference profile $C_0(z)$ shown in figure 2. The upper plot is based on XBT data only, and the bottom plot on acoustic data only. The middle plot is based on the combined XBT and acoustic data.

8. Bias

Consider the rays associated with $C(z)$ in a range-independent ocean, and then generate positive and negative perturbations such that $\langle \delta C(x, z) \rangle = 0$. The first-order perturbation in travel time can be associated with the perturbations in sound speed along the *unperturbed* paths, hence these are proportional to $\langle \delta C(x, y) \rangle$ and will vanish when $\langle \delta C(x, z) \rangle = 0$. But the perturbations $\delta C(x, z)$ will cause perturbations in ray paths, and these give rise to second-order terms which vary as $\langle (\delta C(x, z))^2 \rangle$. Thus it is not clear whether changes in Δ_i, are associated with changes $\langle \delta C(z) \rangle$ in the mean profile, or with a change $\langle (\delta C(x, z))^2 \rangle$ in the intensity of the range-dependent eddy structure (Munk & Wunsch 1985). We hope that the range-dependent information contained in Δ_i will give adequate information to correct for the quadratic bias.

To first order, the perturbation in ray paths is the same in both directions, and there is no corresponding bias problem in reciprocal transmissions leading to $u(z)$.

9. Estimating the eddy fluxes

The sound speed C is nearly a linear function of temperature and only a weak function of salinity. At any point, the time average $F = \overline{uC}$ is then an approximate measure of the heat flux $\overline{uT}$. One-way tomography yields some space and time averages of C; reciprocal tomography measures u. Can the two measurements be combined to yield some interesting averages of the product uC?

Under ideal circumstances, the inversions yield $u(x, z, t)$ and $C(x, z, t)$ and the fluxes can be determined by point-by-point multiplication of the two fields, and subsequent averaging in space–time. The space averages are in the direction of flow. This is a peculiar way of forming flux averages. The usual procedure is to form averages in the direction normal to the flow, such as a mean of poleward heat flux across a fixed latitude. Further, though the mapping of $C(x, z)$ for a 300 km range was moderately successful (see figure 9), this was not so for $u(x, z)$ on account of a larger relative noise level, and will be even more difficult at longer ranges.

We wish to now to return to the spirit of G. I. Taylor: to measure 'the average effect of a collection of eddies' rather than 'the behaviour of eddies considered as individuals'. Consider first the climatological situation:

$$\omega T \ll 1, \quad kR \ll 1,$$

where T is the duration of the experiment and R the range of acoustic transmission. We have in mind $T = 1$ year and $R = 1000$ km. Write

$$C(x, z, t) = C_0(z) + \delta C(x, z, t), \quad u(x, z, t) = u_0(z) + \delta u(x, z, t), \tag{1}$$

with $C_0(z)$, $u_0(z)$ designating the climatological averages, and

$$F_0(z) = u_0(z)\, C_0(z) \tag{2}$$

designating the climatological flux associated with the mean annual flux due to the major ocean gyres. For the present discussion we ignore the considerable complexities associated with the fact that rays are curved, and that the measured ray averages are not the same thing as the range averages $\langle\ \rangle$. The travel times in the $\pm x$-direction are then given by

$$\begin{aligned} \Delta^{\pm}(t) &= \int \frac{\mathrm{d}x}{C \pm u} \approx \frac{1}{C_0} \int \mathrm{d}x \left(1 - \frac{\delta C}{C_0} \mp \frac{u}{C_0}\right) \\ &= \frac{R}{C_0}\left[1 \mp \frac{u_0}{C_0} + \left\langle -\frac{\delta C}{C_0} \mp \frac{\delta u}{C_0} \right\rangle\right). \end{aligned}$$

The time average equals

$$\overline{\Delta^{\pm}(t)} = \frac{R}{C_0^2}(C_0 \mp u_0)$$

since δC and δu are defined to vanish when integrated over R and T. Accordingly

$$F_0 = -\frac{C_0^4}{4R^2}(\overline{\Delta^{+2}} - \overline{\Delta^{-2}}). \tag{3}$$

(As with any 'open' system, such a measurement of the mean flux is not readily interpretable. One must consider a system in which total mass is conserved.)

The departure from the time mean is given by

$$\delta\Delta^{\pm}(t) = -\frac{1}{C_0^2} \int \nu \, \mathrm{d}x, \quad \nu = \delta C \pm \delta u.$$

We form the mean square:

$$\overline{(\delta\Delta^{\pm})^2} = \frac{1}{C_0^4}\int dx_1 \int dx_2\, \overline{\nu(x_1)\,\nu(x_2)}. \tag{4}$$

It has been demonstrated (Mode Group 1978) that for mesoscale currents $\overline{u(x_1)\,u(x_2)} = \overline{u^2}\rho(x_1-x_2)$ with an integral correlation scale

$$r = \int_{-\infty}^{\infty} dx'\,\rho(x'). \quad x' = x_1 - x_2$$

of order 100 km. A similar result is found for temperature. We now boldly assert that

$$\overline{\nu_1\nu_2} = \overline{(\nu)^2}\rho(x'), \quad x' = x_1 - x_2.$$

Writing the integration (4) in terms of sum and difference coordinates $x = \frac{1}{2}(x_1 + x_2)$ and $x' = x_1 - x_2$, we have

$$\overline{(\delta\Delta^{\pm})^2} = \frac{\overline{(\nu^{\pm})^2}}{C_0^4}\int dx \int_{-\infty}^{\infty} dx'\,\rho(x') = \frac{\overline{(\nu^{\pm})^2}}{C_0^4} Rr.$$

It follows that

$$F = \overline{\langle \delta u\, \delta C\rangle} = +\frac{C_0^4}{4Rr}[\overline{(\delta\Delta^{+})^2} - \overline{(\delta\Delta^{-})^2}]. \tag{5}$$

This is computed for each ray i, and the depth-dependent flux $F(z)$ then follows from inversion methods. Note that (5) contains the desired spatial mean product $\langle \delta u\, \delta C\rangle$.

Thus the difference between the squared mean travel times yields the climatological flux $F_0(z)$ (space and time scales large compared to R and T), whereas the difference between the mean-square travel times yields the eddy flux $F(z)$ (associated with small scales). The ideas described in this section are to be tested during the next two years.

10. Acoustic monitoring of ocean gyres

Late this year we shall set three deep-sea moorings forming a 1000 km triangle somewhat north of Hawaii. Each mooring will have a colocated acoustic source and receiver. This experiment will last for one year.

The purpose is to study mean and seasonal properties of the subtropical gyre in the eastern North Pacific. Among these properties are the gyre heat content and (hopefully) the heat flux through the gyre. A new feature is to measure the mean gyre vorticity: travel time from mooring A to B to C to A minus ACBA gives the circulation, which equals the mean vorticity times the area of the triangle ABC. We expect the vorticity to be associated with the population of mesoscale eddies within the triangle. The basic idea is very simple. G.I. will be with us in spirit.

I am very grateful to P. Worcester and B. Howe for permitting the use of unpublished results. This essay is based on a joint effort by the Ocean Acoustic Tomography Group, under the leadership of C. Wunsch of the Massachusetts Institute of Technology, R. Spindel of the Woods Hole Oceanographic Institute, T. Birdsall of the University of Michigan, and P. Worcester and the author at the Scripps Institution of Oceanography. The work is sponsored by the Office of Naval Research and the National Science Foundation.

REFERENCES

HOWE, B. M. 1986 Ocean acoustic tomography: mesoscale velocity. Dissertation, University of California, San Diego: Scripps Institution of Oceanography, La Jolla, CA 92093.

HOWE, B. M., WORCESTER, P. F. & SPINDEL, R. C. 1986 *J. Geoph. Res.* (submitted).

LONGUET-HIGGINS, M. 1982 *Dyn. Atmos. Oceans* **7**, 33–46.

MALANOTTE-RIZZOLI, P. 1985 *J. Geoph. Res.* **90**, 7098–7116.

MODE GROUP 1978 *Deep-Sea Res.* **26**, 123–161.

MUNK, W. H. & WUNSCH, C. 1985 *Deep-Sea Res.* **32**, 1317–1346.

OCEAN TOMOGRAPHY GROUP, THE 1982 *Nature* **299**, 121–125.

ROSSBY, T. R. 1975 *J. Mar. Res.* **33**, 213–222.

SHOCKLEY, R. C., NORTHROP, J. & HANSEN, P. G. 1982 *J. Acoust. Soc. Am.* **71**, 51–60.

TAYLOR, G.I. 1915 *Phil. Trans. R. Soc. Lond.* A**215**, 1–26.

WORCESTER, P. F., SPINDEL, R. C. & HOWE, B. M. 1985 *IEEE J. Oceanic Engng* **OE-10**, 123–137.